# Membrane Lateral Compressibility Determined by NMR and X-Ray Diffraction: Effect of Acyl Chain Polyunsaturation

Bernd W. Koenig*, Helmut H. Strey,# and Klaus Gawrisch*
*Laboratory of Membrane Biochemistry and Biophysics, National Institute on Alcohol Abuse and Alcoholism, and #Laboratory of Structural Biology, Division of Computer Research and Technology, National Institutes of Health, Rockville, Maryland 20852 USA

ABSTRACT The elastic area compressibility modulus, $K_a$, of lamellar liquid crystalline bilayers was determined by a new experimental approach using $^2$H-NMR order parameters of lipid hydrocarbon chains together with lamellar repeat spacings measured by x-ray diffraction. The combination of NMR and x-ray techniques yields accurate determination of lateral area per lipid molecule. Samples of saturated, monounsaturated, and polyunsaturated phospholipids were equilibrated with polyethylene glycol (PEG) 20,000 solutions in water at concentrations from 0 to 55 wt % PEG at 30°C. This procedure is equivalent to applying 0 to 8 dyn/cm lateral pressure to the bilayers. The resulting reductions in area per lipid were measured with a resolution of ±0.2 Å$^2$ and the fractional area decrease was proportional to applied lateral pressure. For 1,2-dimyristoyl$_{d54}$-*sn*-glycero-3-phosphocholine, 1-stearoyl$_{d35}$-2-oleoyl-*sn*-glycero-3-phosphocholine (SOPC-d$_{35}$), and 1-stearoyl$_{d35}$-2-docosahexaenoyl-*sn*-glycero-3-phosphocholine (SDPC-d$_{35}$) cross-sectional areas per molecule in excess water of 59.5, 61.4, and 69.2 Å$^2$ and bilayer elastic area compressibility moduli of 141, 221, and 121 dyn/cm were determined, respectively. Combining NMR and x-ray results enables the determination of compressibility differences between saturated and unsaturated hydrocarbon chains. In mixed-chain SOPC-d$_{35}$ both chains have similar compressibility moduli; however, in mixed-chain polyunsaturated SDPC-d$_{35}$, the saturated stearic acid chain appears to be far less compressible than the polyunsaturated docosahexaenoic acid chain.

## INTRODUCTION

Cell membranes may undergo changes in area per molecule and curvature while maintaining bilayer integrity and fulfilling membrane barrier function. Some membranes are subject to extreme deformation, e.g., the erythrocyte membrane in capillary blood flow, or membranes involved in endo- and exocytosis (Wattenberg, 1992). Furthermore, the lipid matrix may adjust to conformational changes of integral membrane proteins by changing lipid area per molecule and membrane thickness. Membrane lateral compressibility is likely to be important for proper cell function and nature may control it by appropriate membrane composition.

The influence of acyl chain polyunsaturation on membrane properties has been investigated previously (Dratz and Deese, 1986; Salmon et al., 1987; Mitchell et al., 1992; Holte et al., 1995) and there is evidence that membranes rich in transmembrane receptors have particularly high concentrations of polyunsaturated fatty acids (McGee and Greenwood, 1989). For example, the well-studied visual receptor rhodopsin has a specific need for near-native levels of 50 mol % *cis*-polyunsaturated docosahexaenoic acid (22:6n-3) for optimal sensitivity (O'Brian et al., 1977; Miljanich et al., 1979; Wiedmann et al., 1988). The ability of reconstituted membranes to accommodate the transition of rhodopsin from meta I to meta II, which is associated with a volumetric expansion of ~100 cc/mol (Lamola et al., 1974; Attwood and Gutfreund, 1980) depends on the degree of acyl chain unsaturation (Litman and Mitchell, 1996). Dratz and co-workers predict a thickening of the lipid bilayer upon meta II formation (Dratz and Holte, 1992). Litman and co-workers suggested that the extent of meta II formation in rhodopsin may be related to a particularly low lateral compressibility modulus of membranes rich in polyenoic acyl chains, such as docosahexaenoic acid (Mitchell et al., 1992; Litman and Mitchell, 1996).

The current knowledge of elastic properties of lipid bilayers is based primarily on well-established micromechanical studies on single-walled liposomes conducted by Evans and co-workers (Kwok and Evans, 1981; Evans and Kwok, 1982; Evans and Needham, 1987; Needham and Nunn, 1990; Needham, 1995) and analysis of thermal fluctuations of large lipid vesicles (Servuss et al., 1976; Schneider et al., 1984; Faucon et al., 1989; Duwe et al., 1990). Elastic membrane properties have been shown to depend on lipid phase state, temperature, lipid headgroup and hydrocarbon chain composition, and cholesterol content (Evans and Needham, 1987; Needham and Evans, 1988; Needham and Nunn, 1990). Diarachidonylphosphatidylcholine (di-20:4 PC) is the only single-component phospholipid with polyunsaturated acyl chains studied so far (Needham and Nunn, 1990; Evans and Rawicz, 1990). The area expansion modulus of di-20:4 PC bilayers is lower than that of bilayers composed of saturated or monounsaturated lipids. This suggests that polyunsaturation lowers the energy required for elastic membrane deformation.

*Received for publication 6 February 1997 and in final form 11 June 1997.*
Address reprint requests to Klaus Gawrisch, Laboratory of Membrane Biochemistry and Biophysics, National Institute on Alcohol Abuse and Alcoholism, National Institutes of Health, 12420 Parklawn Dr., Rockville, MD 20852. Tel.: (301) 594-3750; Fax: (301) 594-0035; E-mail: gkl@cu.nih.gov

0006-3495/97/10/1954/13 $2.00

Investigations on liposomes composed of highly unsaturated phospholipids require precautions due to sensitivity of polyunsaturated lipids to oxidation and to increased liposome fragility under lateral tension (Needham and Nunn, 1990). This restricts micromechanical experiments to a rather narrow range of low lateral tensions in which measurements are further complicated by bilayer undulations (Evans and Rawicz, 1990). Moreover, the micromechanical technique measures membrane elasticity exclusively by *stretching* the bilayer, thus providing lateral area *expansion* moduli, while under certain conditions the surface could be *compressed.* There may very well be differences in the elastic response of the membrane to lateral compression versus expansion, especially for larger area changes.

Rand and Parsegian suggested an alternative approach to the study of lateral *compressibility* of membranes that makes use of the decrease in membrane area induced by osmotic stress (OS) (Parsegian et al., 1979; Lis et al., 1982). OS will reduce the amount of trapped water between bilayers, which decreases the cross-sectional area per lipid molecule. X-ray diffraction is frequently used to monitor the structural deformations of the membrane unit cell as a function of osmotic stress (Rand and Parsegian, 1989). This technique has the potential to provide, simultaneously, the parameters of the repulsive hydration force acting between opposing bilayers and the lateral area compressibility modulus of the membrane (Parsegian et al., 1979). However, compressibility moduli determined so far by this method (Parsegian et al., 1979; Lis et al., 1982) appeared to be much smaller than the values obtained by micromechanical measurements on liposomes. We and others suggested previously that the Luzzati approach, which was used to calculate the area per lipid molecule from x-ray diffraction data, may exaggerate area changes at water concentrations near excess due to morphological changes in lipid-water dispersions (Gawrisch et al., 1985; McIntosh and Simon, 1986; Klose et al., 1988; Nagle et al., 1996). In the present study we have addressed this problem by determining area changes more precisely by comparing NMR and x-ray results obtained on the same lipid/water samples.

Since the pioneering studies on membrane hydrocarbon chain order by Seelig and co-workers (Seelig and Seelig, 1974, 1980; Schindler and Seelig, 1975; Seelig, 1977) it has been known that lipid order parameters are very sensitive to the smallest changes in area per lipid. Here we demonstrate that NMR is very well suited to measure the small *area changes* induced by osmotic stress. However, calculation of *absolute area values* from NMR data is rather model-dependent (Nagle, 1993). In contrast, x-ray diffraction measurements can provide very precise absolute area values at low lipid hydration by the Luzzati approach if the water content is accurately known, but give unreliable values at higher water concentration (Klose et al., 1988; Nagle et al., 1996). By combining NMR and x-ray data, systematic errors in area determination by either method have been accounted for and lateral compressibility moduli of bilayers were calculated. Comparison of compressibility moduli determined here by the OS technique and area expansion moduli obtained by micromechanical studies indicate good agreement where data are available.

## MATERIALS AND METHODS

The lipids 1,2-dimyristoyl$_{d54}$-*sn*-glycero-3-phosphocholine (diMPC-$d_{54}$) and 1-stearoyl$_{d35}$-2-oleoyl-*sn*-glycero-3-phosphocholine (SOPC-$d_{35}$) were obtained from Avanti Polar Lipids, Inc. (Alabaster, AL). 1-stearoyl$_{d35}$-2-docosahexaenoyl-*sn*-glycero-3-phosphocholine (SDPC-$d_{35}$) was purchased from Matreya, Inc. (Pleasant Gap, PA). To minimize oxidation of SDPC-$d_{35}$, the manufacturer added butylated hydroxytoluene (BHT) at a molar lipid-to-BHT ratio of 250:1. Representative lots of lipids were checked for purity by analytical high-performance liquid chromatography (HPLC). Lipids initially dissolved in chloroform or methylene chloride were dried in a stream of argon, redissolved in cyclohexane, frozen, and lyophilized overnight in the dark to give a fluffy powder. In the case of SDPC-$d_{35}$ all manipulations were carried out in a glove box under argon.

Polyethylene glycol (PEG) with a molecular weight of $\geq$17,000 (PEG20,000) was purchased from Fluka, Switzerland. At a temperature of 30°C the polymer is water-soluble up to ~60 wt % PEG. Osmotic pressure, $\Pi$, of aqueous PEG solutions was calculated from the concentration dependence established by Parsegian et al. (1986):

$$\log \Pi = 1.57 + 2.75\ \omega^{0.21} \qquad (1)$$

where $\Pi$ is in dyn/cm$^2$ and $\omega$ is the weight percent polymer. The coefficients in Eq. 1 represent a recent refinement and were provided by Dr. P. Rand (Brock University, Ontario, Canada; http://aqueous.labs.brocku.ca/data/peg20000). By using solutions with 7–55 wt % PEG, the range of osmotic pressure covered is $5.1 \times 10^5 < \Pi < 8.9 \times 10^7$ dyn/cm$^2$. PEG was dissolved in deuterium-depleted water (Isotec, Inc., Miamisburg, OH). Sodium azide (0.02 wt %) was added to prevent bacterial growth and 125 $\mu$M diethylenetriaminepentaacetate to minimize lipid oxidation induced by catalytic action of multivalent ions. PEG solutions were sealed in vials and stored in an incubator at 30°C for 6 h to completely dissolve the PEG. Solutions were stirred with a glass rod before introducing the lipid.

### Sample preparation

Dialysis bags (MW cutoff at 8000; SPECTRUM, Houston, TX) containing 15 mg prehydrated lipid were submerged into 1.5 ml PEG solution in a vial. Sealed vials were equilibrated at 30 $\pm$ 0.5°C for 48 h. Equilibrated lipid/water mixtures were divided into samples for proton (2 mg) and $^2$H-NMR measurements (10 mg). About 50 mg of the PEG solution were added to the $^2$H-NMR sample. The weight of the sealed vials and sample tubes did not change with time, confirming a good seal. After the $^2$H-NMR experiments the lipid/PEG mixtures were transferred into capillary tubes for x-ray diffraction (Fa. W. Müller, Berlin, Germany). Capillary tubes were sealed with a paraffin plug and an epoxy coating.

### $^1$H-NMR MAS measurement of water concentration

$^1$H-NMR spectra of lipid/water mixtures were recorded on a Bruker DMX500 spectrometer using magic angle spinning (MAS) at 5 kHz. A total of 16 scans were accumulated at a rate of one scan per 10 s. At 30°C, the proton signals from water and lipid choline are well resolved (linewidth of 20 Hz). Both signals have negligible sideband intensities. Integral intensities of both signals in the center band were determined by peak fitting after exponential line broadening (20 Hz) and a polynomial baseline correction. The molar water-to-lipid ratio in the sample, $R_{W/L}$, was calculated from the integral intensities of the water ($I^{water}$) and choline-methyl

($I^{choline}$) peaks, respectively.

$$R_{W/L} = \frac{9}{2}\frac{I^{water}}{I^{choline}}. \quad (2)$$

The procedure described is applicable only for PEG-free lipid/water dispersions. This requirement was met by using dialysis bags during equilibration. The typical precision of this water concentration measurement is better than ±0.5 water molecules per lipid.

## Bilayer dimensions from $^2$H-NMR order parameters

$^2$H-NMR spectra were observed on a Bruker DMX300 spectrometer at 46.1 MHz using a high-power probe with a 5-mm solenoid sample coil. A quadrupolar echo pulse sequence (Davis, 1983) with a 2-$\mu$s 90° pulse, a 50-$\mu$s delay between pulses, a repetition rate of two acquisitions per second, and a spectral width of 200 kHz were used to acquire the data. The carrier frequency was placed exactly at the center of the spectrum. Free induction decays were left-shifted to ensure that the Fourier transform began exactly at the echo maximum. A Bruker variable-temperature unit was used to maintain sample temperature at 30 ± 0.1°C. Before data accumulation samples were equilibrated at the experimental temperature for at least 30 min.

The effective length, $\langle L \rangle$, of a perdeuterated lipid acyl chain in a liquid crystalline, $L_\alpha$, phase bilayer was calculated from the $^2$H-NMR order parameters. Briefly, the $^2$H-NMR spectrum of lipid specifically labeled at the $n$th carbon position in a membrane oriented with its bilayer normal perpendicular to the magnetic field, $B_0$, consists of two sharp peaks separated by the quadrupole splitting $\Delta\nu_Q$:

$$\Delta\nu_Q = \frac{3}{4}\frac{e^2qQ}{h}S(n), \quad (3)$$

where $e^2qQ/h$ is the quadrupole coupling constant (167 kHz for $^2$H in a C—$^2$H bond) and $S(n)$ is the time-averaged orientational order parameter of the deuterium-labeled segment.

$$|S(n)| = \frac{1}{2}\langle 3\cos^2\theta_n - 1\rangle. \quad (4)$$

The averaging accounts for motions of the carbon—deuterium bond occurring with correlation times of $10^{-5}$ s and faster. $\theta_n$ is the angle between the carbon—deuterium bond vector and the bilayer normal.

$^2$H-NMR powder pattern spectra of perdeuterated lipid acyl chains were dePaked (Sternin et al., 1983; McCabe and Wassall, 1995) to give spectra that correspond to the 0° orientation of the lipid bilayer normal with respect to $B_0$. Smoothed order parameter profiles were calculated according to Lafleur et al. (Lafleur et al., 1989; Holte et al., 1995). For the purpose of chain length calculation, the experimental order parameter of the terminal methyl group was replaced by an extrapolation from a linear fit to the order parameters of the two methylenes immediately preceding the methyl (Lafleur et al., 1989). The projection length, $\langle L \rangle$, of the chain on the bilayer normal is a linear function of the average order parameter, $\langle S \rangle$, according to semi-empirical models initially developed by Seelig et al. (Seelig and Seelig, 1974; Schindler and Seelig, 1975):

$$\langle L \rangle = 1(0.5 + \langle |S| \rangle). \quad (5)$$

The length $l$ amounts to $l = n \times 1.27$ Å, where $n$ is the number of C—C bonds in a single perdeuterated acyl chain, and 1.27 Å is the distance between two carbon atoms projected on the long axis of the all-*trans* reference state (Bunn, 1939).

We define the hydrocarbon core of a membrane unit cell to contain all and only the hydrocarbon chains of two lipid molecules. Its volume, $V_{HC}$, was calculated by summation over the individual $CH_3$, $CH_2$, and CH segments, which occupy 54.0, 27.0, and 20.5 Å$^3$, respectively, in the $L_\alpha$ phase (Marsh, 1992). The thickness of the hydrocarbon core, $d_{HC}^{NMR}$, is

$$d_{HC}^{NMR} = 2\langle L \rangle. \quad (6)$$

Calculation of the cross-sectional area per lipid molecule in the lipid/water interface, $A^{NMR}$, is straightforward:

$$A^{NMR} = V_{HC}/d_{HC}^{NMR}. \quad (7)$$

Calculation of parameters $d_{HC}^{NMR}$ and $A^{NMR}$ according to Eqs. 6 and 7 ignores chain upturns and interdigitation (Nagle, 1993). Furthermore, it is assumed that *sn*-1 and *sn*-2 chains have the same average geometrical length.

## Bilayer dimensions from x-ray diffraction

The repeat spacing, $d$, of multilamellar lipid vesicles in the $L_\alpha$ phase was determined by x-ray diffraction using an Elliot GX-13 rotating-anode x-ray generator equipped with two x-ray mirrors and a Frank-type camera. Kodak image plates were used for detection. They were scanned and digitized by a Phosphor Imager SI (Molecular Dynamics, CA). Diffraction patterns consisted of up to four equally spaced circles characteristic of a single lamellar phase. The radial scattering intensity was determined using the program NIH IMAGE, version 1.60 (W. Rasband, National Institutes of Health, Bethesda, MD) modified by H.H.S. The molecular volume of diMPC, SOPC, and SDPC was calculated to be 1106, 1286, and 1361 Å$^3$, respectively, using a specific volume of 0.983 cm$^3$/g reported for comparable lipids (Nagle and Wilkinson, 1978; White et al., 1987).

If the water concentration in the multilamellar membrane stacks is identical to the molar lipid-to-water ratio in the sample, $R_{W/L}$, the cross-sectional area per lipid molecule in the lipid/water interface, $A^{x\text{-}ray}$, can be calculated according to:

$$A^{x\text{-}ray} = (V_L + V_W)/d, \quad (8)$$

where $V_L$ is the volume of two lipid molecules and $V_W$ is the water volume calculated from twice the number of water molecules per lipid, $R_{W/L}$. The thickness of the water layer between apposing bilayers, $d_W$, was calculated by the gravimetric method proposed by Luzzati (Luzzati, 1968; Rand et al., 1988).

## Elastic area compressibility modulus

The area occupied per lipid molecule in the plane of the bilayer, $A$, is determined by the isotropic lateral bilayer tension, $\tau$. Area, $A_0$, is the corresponding value for bilayers in excess water, a stress-free state. It is convenient to express area changes in terms of the fractional change, $\alpha$:

$$\alpha = \frac{A - A_0}{A_0}. \quad (9)$$

In general, the slope of $\tau$ versus $\alpha$ may vary with the lateral tension exerted on the membrane. However, within the elastic limit of deformation, i.e., for small $\alpha$, the slope is constant and represents the isothermal elastic area compressibility modulus, $K_a$:

$$K_a = A_0\left(\frac{\partial\tau}{\partial A}\right)_T = \left(\frac{\partial\tau}{\partial\alpha}\right)_T. \quad (10)$$

For constant $K_a$ Eq. 10 is equivalent to

$$K_a(A - A_0) = A_0\tau \quad (11)$$

The bilayer tension, $\tau$, is related to the osmotic pressure, $\Pi$, of the PEG solution (see Appendix):

$$\tau = -2v_W \frac{R_{W/L}}{A} \Pi, \quad (12)$$

where $v_W$ is the molecular volume of water. Note that both $\tau$ and $\alpha$ assume negative values in the regime of membrane compression, accessible with the OS technique. In what follows, the absolute value of $\tau$ will be referred to as lateral surface pressure sensed by a lipid molecule in the bilayer, since this term is more intuitive for the compression regime.

The functional dependence between $A$ and the water activity, $a_W$, can be obtained by substituting $\tau$ in Eq. 11 according to Eq. 12 and recalling that $\Pi = -(kT/v_W)\ln a_W$. The subsequent expansion to series of the square root provides an approximation, which works well if area changes are below 20%.

$$A = A_0\left(1 + \frac{2R_{W/L}kT \ln a_W}{A_0 K_a}\right) \quad (13)$$

Determination of the two free parameters, $A_0$ and $K_a$, was performed by application of a Nelder–Mead nonlinear least-squares algorithm, which explicitly accounts for uncertainty in both independent and dependent variables (Johnson and Frasier, 1985; Johnson, 1985). Asymmetric confidence intervals corresponding to one standard deviation were estimated for both parameters. However, due to the minimal observed asymmetry for $A_0$, a single value of uncertainty is reported for this parameter.

## RESULTS AND DISCUSSION

### Kinetics of sample equilibration

The central point in the reliable determination of membrane properties by the OS technique is to ensure thermodynamic equilibrium between polymer solution and lipid phase at the time of the measurements. The time required to reach equilibrium was determined experimentally. Fully hydrated diMPC-$d_{54}$ samples were incubated with an excess of PEG solution in the NMR probe. A series of $^2$H-NMR spectra with an accumulation time of 30 min each was recorded and the average chain order parameters, $\langle S \rangle$, were calculated. $^2$H-NMR order parameters are very sensitive to small changes in bilayer structure caused by changes in lipid hydration. Equilibration curves for diMPC-$d_{54}$ in *direct contact* with aqueous PEG solutions at high, intermediate, and low polymer concentrations at $T = 30 \pm 0.1$°C are shown in Fig. 1. After 5 to 10 h the average order parameter becomes constant, confirming that lipid hydration reached thermodynamic equilibrium. Additional NMR experiments on diMPC-$d_{54}$ samples equilibrated in *dialysis bags* confirmed that equilibrium water distribution was reached within one day. An equilibration time of 48 h was used in the experiments described below.

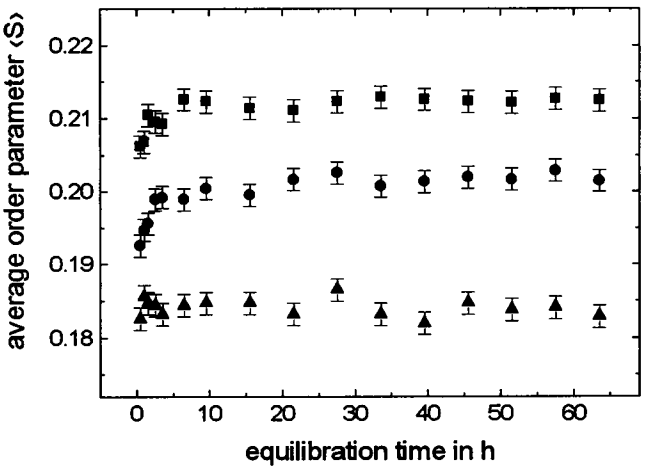


FIGURE 1 Average $^2$H-NMR chain order parameter, $\langle S \rangle$, of diMPC-$d_{54}$ multilamellar liposomes as a function of equilibration time. Initially the lipid was fully hydrated. The lipid was kept in direct contact with an excess of PEG solution at $T = 30 \pm 0.1$°C and $^2$H-NMR spectra were recorded over a period of three days. ■, 50 wt % PEG 20,000, $a_W = 0.953$; ●, 43 wt % PEG 20,000, $a_W = 0.970$; ▲, 10 wt % PEG 20,000, $a_W = 0.999$.

### Water sorption isotherms

The overall molar water-to-lipid ratio in the lipid dispersions after equilibration as a function of the water activity, $a_W$, is shown in Fig. 2. The data represent the sorption isotherms of diMPC-$d_{54}$, SOPC-$d_{35}$, and SDPC-$d_{35}$ at 30°C in the region of high water activity ($0.93 < a_W < 1$). The shape of the curves qualitatively resembles water sorption behavior of other phosphatidylcholine lipids in the $L_\alpha$ phase, for example egg PC (Jendrasiak and Hasty, 1974) and 1-palmitoyl-2-oleoylphosphatidylcholine (Klose et al., 1992). No difference in water sorption behavior was found between diMPC-$d_{54}$ and SOPC-$d_{35}$ over the $a_W$ range studied. However, SDPC-$d_{35}$ adsorbs more water than the two other lipids at all water activities. In a previous study on phosphatidylcholines with up to four double bonds per lipid it was also found that the adsorption of water by $L_\alpha$ phase lipids increases with the number of double bonds in the lipid acyl chains (Jendrasiak and Hasty, 1974). It should be noted that our measurements on SDPC-$d_{35}$ at the highest water

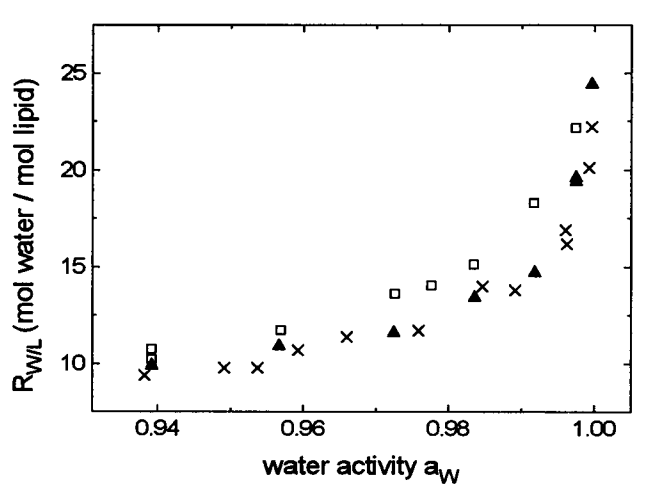


FIGURE 2 Water sorption isotherms of diMPC-$d_{54}$ (×), SOPC-$d_{35}$ (▲), and SDPC-$d_{35}$ (□) at $T = 30$°C. The ratio of water to lipid (mol/mol) in the sample was measured after thermodynamic equilibrium had been established with an excess amount of PEG solution.

activity studied, $a_W = 0.99964$, gave values for $R_{W/L}$ between 37 and 55, but lacked reproducibility. At these higher water concentrations the forces acting between bilayers are weak and the net energy potential minimum that determines bilayer separation is shallow, which may result in an influence of sample handling on water uptake. Those data points at high water activity were not used for subsequent processing.

## Water distribution within the sample and area per molecule

The precise measurement of relative changes in area per lipid molecule, $A$, as a function of applied osmotic stress is crucial for determination of bilayer area compressibility.

The average $^2$H-NMR order parameter, $\langle S \rangle$, is very sensitive to *changes* in the time averaged projection lengths, $\langle L \rangle$, of the acyl chain and its cross-sectional area, $A^{NMR}$. The detection threshold for changes in $\langle L \rangle$ and $A^{NMR}$ is <0.5% (Ipsen et al., 1990; Holte et al., 1996). This high sensitivity is needed for determination of lateral compressibility. Another advantage of the NMR approach is that calculation of $A^{NMR}$ does not require knowledge of the water-to-lipid ratio in the multilamellar membrane stacks. Even the highest osmotic stress applied in this study produced only a modest increase in $d_{HC}^{NMR}$ of 1.3 Å (diMPC-$d_{54}$), 1.1 Å (SOPC-$d_{35}$), and 0.7 Å (SDPC-$d_{35}$), while $A^{NMR}$ decreased by 3.5 Å$^2$ (diMPC-$d_{54}$), 2.5 Å$^2$ (SOPC-$d_{35}$), and 1.8 Å$^2$ (SDPC-$d_{35}$), compared to the unstressed state. These total changes are close to, or even smaller than, the resolution of conventional scattering density profiles obtained from x-ray or neutron diffraction on model membranes in the $L_\alpha$ phase (McIntosh and Simon, 1986; Wiener and White, 1991; Nagle et al., 1996). The increments of area expansion as a function of water concentration, $R_{W/L}$, become smaller with increasing water content. The cross-sectional area per lipid molecule in excess water, $A_o^{NMR}$, was found to be the same as the value determined at the lowest PEG concentration investigated (7 wt %), within experimental uncertainty.

X-ray measurements permit determination of the repeat spacing, $d$, with high precision (±0.2 Å). However, the calculation of $A^{x\text{-}ray}$ by the Luzzati approach, Eq. 8, requires precise knowledge of the water concentration in the multilamellar membrane stack. This prevents calculation of the area per lipid molecule in the presence of excess water by this approach. The Luzzati method may already give false results when the water content of the sample is close to excess water. It is important to realize that the overall water-to-lipid ratio of the sample (Fig. 2) does not necessarily apply to individual bilayer stacks. Previous studies on phosphatidylcholine lipids in the $L_\alpha$ phase suggest that only the first 15 water molecules per lipid are homogeneously incorporated (Gawrisch et al., 1985). Upon addition of more water, an increasing fraction of water forms pockets apart from the neatly stacked multibilayer lattice, e.g., located in the center of budding multilamellar vesicles or between neighboring vesicles (cf. Fig. 3), causing gradual changes in the morphology of the sample (Klose et al., 1988). The presence of these water pockets prevents calculation of meaningful $A^{x\text{-}ray}$ values by the Luzzati method (Eq. 8).

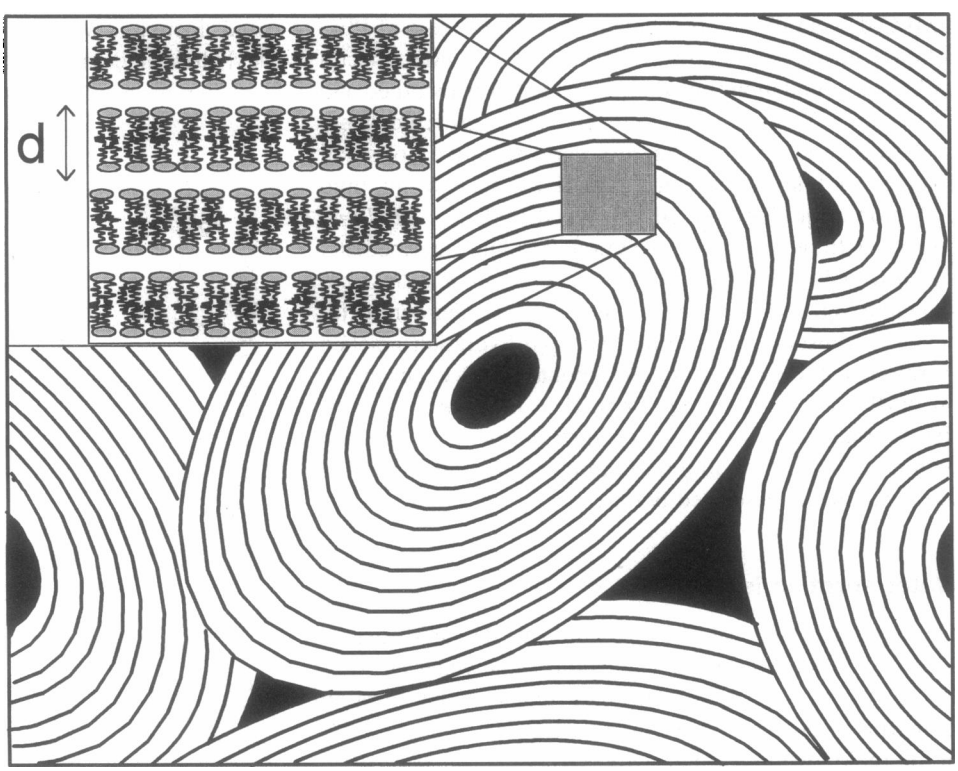


FIGURE 3 An illustration of the discrepancy between overall water content in the sample and water concentration in multilamellar membrane stacks. Formation of multilamellar liposomes also results in formation of water-filled packing defects. Water pockets may exist, e.g., in the center of liposomes and between liposomes (*sketched in black*). In x-ray data analysis by the gravimetric Luzzati method, the existence of such water pockets is neglected.

Areas calculated from NMR and x-ray data are shown in Fig. 4. The diMPC-$d_{54}$ and SOPC-$d_{35}$ results will be discussed first. The $A^{x\text{-}ray}$ values appear to be a linear function of $a_W$ for $R_{W/L}$ up to ~15 waters per lipid and are very nonlinear for higher water content. $A^{NMR}$ values (*filled squares*) calculated according to Eqs. 5–7 are systematically higher than the $A^{x\text{-}ray}$ values (*open squares*). In contrast to the x-ray data, $A^{NMR}$ is proportional to $a_W$ over the entire range of $a_W$ studied. The functional relationship between the cross-sectional area per lipid, $A$, and the water activity, $a_W$, depends on the repulsive hydration forces acting between lipid bilayers. It was shown previously (Rand and Parsegian, 1989) that the hydration force as a function of interbilayer water content per lipid, $V_W = R_{W/L}v_W$, can be approximated by an exponential function, $\Pi = P_0\exp(-V_W/\mu)$, where $P_0$ is the hydration repulsion at zero water volume, and $\mu$ a decay volume. Based on the identity $\Pi = -(kT/v_W)\ln a_W$, this relation can be used to express $R_{W/L}$ as a function of $a_W$:

$$R_{W/L} = -\frac{\mu}{v_W}\ln\left(-\frac{kT}{v_W P_0}\ln a_W\right) \qquad (14)$$

Inserting this relation into Eq. 13 yields a unique functional dependence between $A$ and $a_W$. Analysis of the resulting expression shows that over the range of water activities from 0.94 to 1.0 the area per molecule is an almost linear function of water activity. The deviation of area values from linearity is smaller than 0.3%, which is negligible compared to experimental errors.

The slope of the linear regression line through the NMR data is identical within experimental error to the slope through the x-ray data at $R_{W/L} < 15$. Identical slope of NMR and x-ray curves indicates that the *relative* area change of the deuterated acyl chains matches the *relative* change of the cross-sectional area per lipid calculated from x-ray data.

It is expected that the Luzzati approach provides reliable area values at low water content ($R_{W/L} < 15$) since no inhomogeneous water distribution was found for similar phosphatidylcholine membranes in this $R_{W/L}$ range (Gawrisch et al., 1985; Klose et al., 1988). Therefore, the discrepancy between absolute values of $A^{NMR}$ and $A^{x\text{-}ray}$ at $R_{W/L} < 15$ is most likely the result of an overestimation of $A^{NMR}$. An overestimation of $A^{NMR}$ was also confirmed for chain perdeuterated dipalmitoylphosphatidylcholine, diPPC-$d_{62}$. In excess water at 50°C we calculated an $A^{NMR}$ per diPPC-$d_{62}$ molecule of 68 Å$^2$, which is 5.1 Å$^2$ higher than the 62.9 ± 1.3 Å$^2$ determined recently by Nagle et al. (1996) for diPPC under identical conditions from high-resolution diffraction data. These findings are not surprising since Eqs. 5 to 7, used for calculation of $A^{NMR}$, have been derived under grossly simplified assumptions. To avoid the assumption that the average chain length is precisely half the bilayer thickness, Nagle (1993) suggested using only order parameters of the order parameter plateau (upper half of hydrocarbon chain) for calculation of lipid area per molecule. Indeed, Nagle's procedure results in good agreement between $A^{NMR}$ and $A^{x\text{-}ray}$ data for the saturated diPPC and diMPC. However, for unsaturated lipids we obtained $A^{NMR} < A^{x\text{-}ray}$ when using this approach. The difference increases from SOPC-$d_{35}$ to SDPC-$d_{35}$. Therefore it is likely that accurate calculation of $A^{NMR}$ for mixed-chain

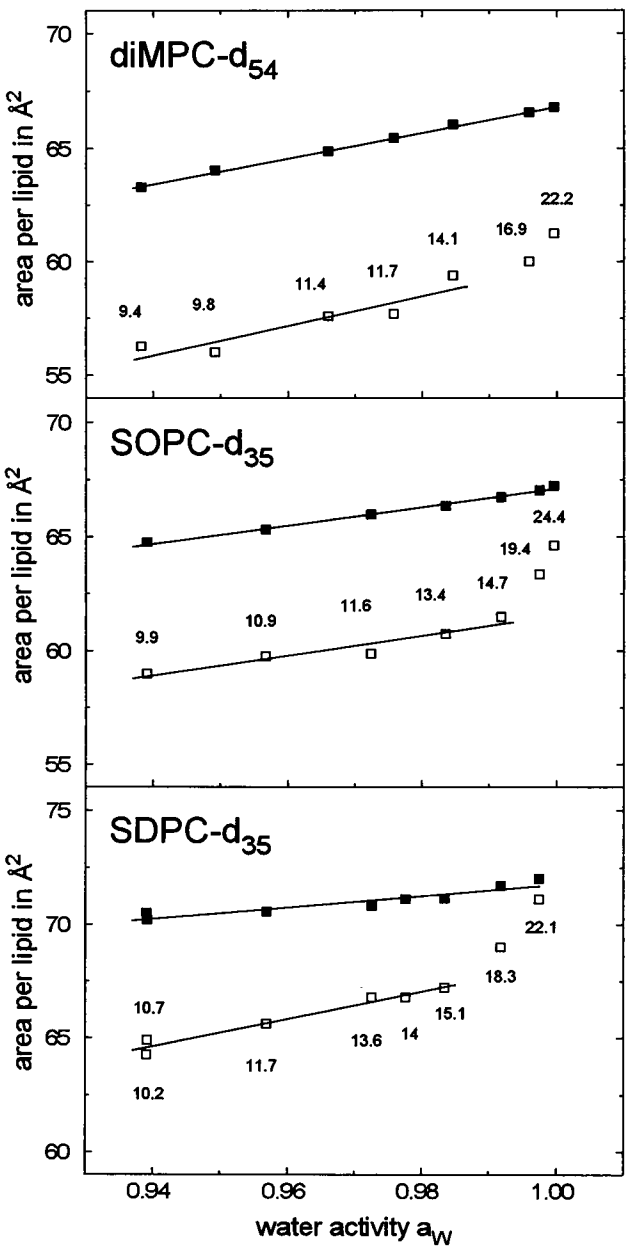


FIGURE 4 Area per lipid molecule perpendicular to the bilayer normal as a function of water activity for diMPC-$d_{54}$, SOPC-$d_{35}$, and SDPC-$d_{35}$ at $T$ = 30°C. Area values were calculated from x-ray (*open squares*, Eq. 8) and NMR data (*filled squares*, Eq. 7). Measurements were performed on the same samples. The molar water-to-lipid ratio is given next to the x-ray data points. Lines represent linear regression of all the NMR data points or of low-water-content x-ray data points, respectively. The apparent discrepancy between NMR and x-ray based raw data presented here is the result of systematic errors and is addressed in the body of the manuscript.

unsaturated phospholipids requires consideration of additional factors.

The difference between $A^{NMR}$ and $A^{x\text{-}ray}$ for $R_{W/L} < 15$ is on average 7.5 and 5.8 Å$^2$ for diMPC-$d_{54}$ and SOPC-$d_{35}$, respectively. An empirical correction can be applied to $A^{NMR}$ to ensure coincidence of x-ray- and NMR-derived areas for $R_{W/L} < 15$, e.g., by subtracting an appropriate constant or by applying a scaling factor.

Comparison of $A^{x\text{-}ray}$ and $A^{NMR}$ values obtained from the same samples allows estimation of the water concentration limit up to which water is completely located in bilayer stacks. Deviation from the expected linear relationship between $a_W$ and $A^{x\text{-}ray}$ at high water activity in contrast to the observed proportionality between $a_W$ and $A^{NMR}$ can be used as an empirical criterion to determine this limit. The data in Fig. 4 indicate that for diMPC-$d_{54}$ and SOPC-$d_{35}$, homogeneous water distribution throughout the samples prevails up to $R_{W/L} \approx 15$. $A^{x\text{-}ray}$ values calculated by Eq. 8 for samples with higher water content are probably too large and have no structural meaning. We cannot exclude the possibility that the method of sample preparation has some influence on the limiting $R_{W/L}$-value, beyond which application of the Luzzati method provides erroneously large $A^{x\text{-}ray}$ values.

Similar to the saturated and monounsaturated lipids, the polyunsaturated SDPC-$d_{35}$ (Fig. 4, *lower panel*) also shows a linear relation between $a_W$ and $A^{NMR}$ over the $a_W$ range studied, while the range for a linear dependence between $a_W$ and $A^{x\text{-}ray}$ is again restricted to $R_{W/L}$ values up to about 15. However, the slopes of the regression lines through $A^{NMR}$ and $A^{x\text{-}ray}$, which are a measure of the area change upon increase of $a_W$, are clearly different. At this point it is important to remember that $^2$H-NMR reports the area change of the *sn*-1 hydrocarbon chain while x-ray diffraction reports area changes of the entire membrane unit cell, which includes both the *sn*-1 and *sn*-2 acyl chains of the lipid. Therefore, the different slopes may indicate that under lateral pressure, saturated and polyunsaturated hydrocarbon chains undergo rather different area changes. Alternatively, a systematic increase with increasing water activity of the amount of water transiently present in the bilayer hydrocarbon core may occur.

Let us first discuss the hypothesis of nonequivalent fractional area changes for the *sn*-1 and *sn*-2 chains. A schematic illustration for this scenario is given in Fig. 5. In order to account for the larger change in $A^{x\text{-}ray}$, the decrease in cross-sectional area upon dehydration has to be greater for the (22:6n-3) chain than for the (18:0) chain. This requires a variable degree of dynamic interdigitation of acyl chains from adjacent monolayers at the center of the bilayer. Involvement of just a few hydrocarbon segments at the terminal end of the acyl chains in the interdigitation would be sufficient to account for the nonequivalent slopes between $A^{x\text{-}ray}$ and $A^{NMR}$ regression lines in Fig. 4. Finally, if this model applies, then the lateral compressibility modulus of the polyunsaturated chain would be smaller than that of the saturated chain.

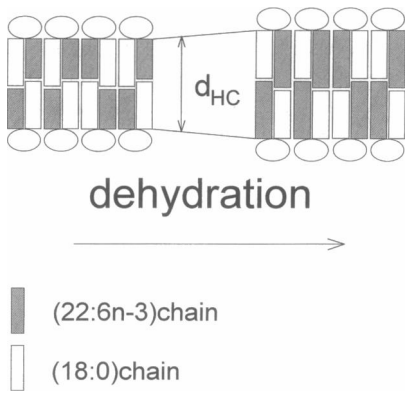


FIGURE 5 Schematic representation of differences in the response of stearoyl and docosahexaenoyl chains of SDPC-$d_{35}$ to membrane dehydration, which increases lateral pressure. Small changes in length of the saturated chain are accompanied by larger changes in the polyunsaturated docosahexaenoic acid chain. Differences in lateral compressibilities between saturated and polyunsaturated chains may result in variable degrees of chain interdigitation.

The alternative interpretation relies on the fact that $A^{x\text{-}ray}$ represents the net cross-sectional area of the membrane unit cell. It includes contributions from either one of the two acyl chains and water, if present in the hydrocarbon region, without differentiating between the components. A redistribution of water from the interbilayer water gap to the interior of the bilayer would result in a smaller repeat spacing, $d$, and larger $A^{x\text{-}ray}$ (Eq. 8). In contrast, $A^{NMR}$ is based entirely on the average motional order of the deuterated acyl chain and does not explicitly account for water molecules transiently present in the membrane interior. Under these conditions the larger increase of $A^{x\text{-}ray}$ with increasing $a_W$ could be the result of variable amounts of water in the bilayer hydrocarbon core. If we apply this scenario and assume that *sn*-1 and *sn*-2 chains have identical chain length, then over the $a_W$ range from 0.94 to 1 our data would translate into a volume gain in the interior of the membrane equivalent to 1.5 water molecules per lipid. This appears to be a large number, even though fluorescence lifetime studies on hydrophobic probes indicate a somewhat increased probability for the presence of water in membranes if they contain polyunsaturated lipids (Straume and Litman, 1987a; Mitchell et al., 1992). Therefore, we consider nonequivalent fractional area changes for the *sn*-1 and *sn*-2 chains without incorporation of significant amounts of water into the membrane hydrophobic core to be a more likely explanation for the difference in slope between the $A^{NMR}$ and $A^{x\text{-}ray}$ data for SDPC-$d_{35}$ in Fig. 4.

Area-per-lipid data obtained at restricted water content, where Eq. 8 gives structurally meaningful $A^{x\text{-}ray}$ values, are shown in Fig. 6. The area per lipid molecule increases with increasing degree of unsaturation in the *sn*-2 acyl chain, i.e., $A$(diMPC) < $A$(SOPC) < $A$(SDPC). However, we cannot exclude the possibility that differences in the number of carbon atoms per chain are partially responsible for the

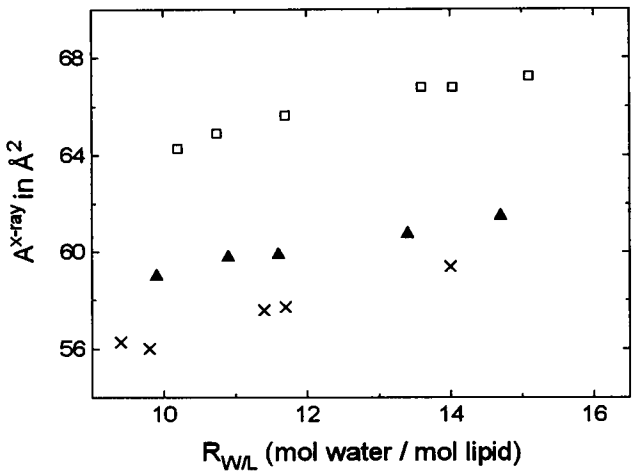


FIGURE 6 Area per lipid molecule perpendicular to the bilayer normal as a function of water concentration for diMPC-$d_{54}$ (×), SOPC-$d_{35}$ (▲), and SDPC-$d_{35}$ (□) samples at $T$ = 30°C. Data were calculated from x-ray measurements by the Luzzati method. Analysis was restricted to samples with low water content, where application of Eq. 8 is appropriate.

observed trend [see, e.g., Morrow et al. (1992); Marsh (1996)].

## Area compressibility from NMR data

In Fig. 7 the lateral pressure sensed by a lipid in the bilayer, $\tau$, is plotted as a function of the fractional area change, $\alpha$, which was calculated according to Eq. 9 using the $A^{NMR}$ values (left side of Fig. 7). The experimental data indicate a *linear* relationship between $\alpha$ and $\tau$ over the entire range of osmotic pressure studied for all three lipids.

Consequently, application of Eq. 13 is justified for data analysis. The two free parameters, $A_0$ and $K_a$, were estimated by a nonlinear least-squares fit of the experimental data ($A = A^{NMR}$, $R_{W/L}$, and $a_W$). Lateral compressibility moduli of 136 (123 to 152) dyn/cm (diMPC-$d_{54}$), 220 (210 to 230) dyn/cm (SOPC-$d_{35}$), and 307 (259 to 371) dyn/cm (SDPC-$d_{35}$) were obtained. The asymmetrical confidence intervals given in parentheses correspond to one standard deviation.

Using $A^{NMR}$ values that were empirically corrected by subtracting a constant (7.5 Å$^2$ for diMPC-$d_{54}$; 5.8 Å$^2$ for SOPC-$d_{35}$) did not change the $K_a$ values. However, applying a factor to scale the absolute $A^{NMR}$ values such that they match the x-ray data at $R_{W/L} \leq 14$ yielded $K_a$ values that were increased by ~10%. Correction of the absolute values of $A^{NMR}$ is important for obtaining meaningful $A_0$ values. The two types of corrections applied gave almost identical results of 59.5 ± 0.2 Å$^2$ for diMPC-$d_{54}$ and 61.4 ± 0.2 Å$^2$ for SOPC-$d_{35}$. Any attempt to empirically correct the $A^{NMR}$ values of SDPC-$d_{35}$ is likely to be flawed due to the nonidentical slope of ($A^{NMR}$ versus $a_W$) and ($A^{x\text{-}ray}$ versus $a_W$) at low hydration (Fig. 4) and was therefore not attempted. Nevertheless, our findings for diMPC-$d_{54}$ and SOPC-$d_{35}$ suggest that correction of $A^{NMR}$ would have only a rather small influence on $K_a$ of SDPC-$d_{35}$.

The $K_a$ values derived from NMR data represent the elastic area compressibility moduli of the *saturated acyl chains* of the lipids studied. The deuterated *sn*-1 chain in SDPC-$d_{35}$ is the one least deformable by lateral pressure even though it has the lowest average $^2$H-NMR order parameter, indicating lower orientational order and larger area compared to the other two lipids. The latter observation is in agreement with previous studies on mixed chain phosphatidylcholines with a saturated *sn*-1 chain and varying unsaturation in the *sn*-2 position. At constant temperature a systematic decrease in the average $^2$H-NMR order parameter of the saturated chain with increasing degree of unsaturation in *sn*-2 was reported (Holte et al., 1995).

Determination of the cross-sectional area values, $A^{NMR}$, used for calculation of $K_a$ is independent of $R_{W/L}$. Nevertheless, inaccurate knowledge of the water-to-lipid ratio in the bilayer stacks has some influence on $K_a$ due to the dependence of $\tau$ on $R_{W/L}$ (Eq. 12). However, the suspected overestimation of $R_{W/L}$ at high water content, which we discussed above, would only insignificantly alter the $K_a$ values because $\tau$ is close to zero at high water content anyway.

## Area compressibility from x-ray data

Areas per lipid determined by x-ray diffraction were used to calculate lateral pressure, $\tau$, and fractional area change, $\alpha$. Only data points with $R_{W/L} \leq 14$ were used for determination of $K_a$. This restrictive criterion was applied to rule out any possible influence of overestimated $A^{x\text{-}ray}$ values on the compressibility moduli. Relaxing the criterion to $R_{W/L} \leq 16$ would alter the $K_a$ values somewhat; however, the changes are within experimental error. A linear correlation between $\tau$ and $\alpha$ was observed (Fig. 7) and Eq. 13 was used to determine $A_0$ and $K_a$ based on a nonlinear least-squares fit of the experimental data ($A = A^{x\text{-}ray}$, $R_{W/L}$, and $a_W$). Lateral compressibility moduli of 141 (91–260) dyn/cm, 221 (165–336) dyn/cm, and 121 (95–161) dyn/cm and $A_0$ values of 59.5 ± 1 Å$^2$, 61.4 ± 0.6 Å$^2$, and 69.2 ± 0.9 Å$^2$, were obtained for diMPC-$d_{54}$, SOPC-$d_{35}$, and SDPC-$d_{35}$, respectively.

In contrast to the $^2$H-NMR experiments, for x-ray data, the slope of the regression line in Fig. 7 (*right side*) represents the area compressibility modulus, $K_a$, of the *bilayer*. The reasonable agreement between $K_a$ values from NMR and x-ray data for diMPC-$d_{54}$ and SOPC-$d_{35}$ is the result of almost identical changes in area seen by both methods. The large difference in compressibility between the stearoyl chain of SDPC-$d_{35}$ ($K_a$ = 307 dyn/cm, determined by $^2$H-NMR) and the entire SDPC-$d_{35}$ bilayer ($K_a$ = 121 dyn/cm, determined by x-ray diffraction) has been addressed in the discussion of Fig. 4 in the paragraph on area per molecule.

Use of x-ray data points in the analysis for which application of the Luzzati approach (Eq. 8) yields artificially high

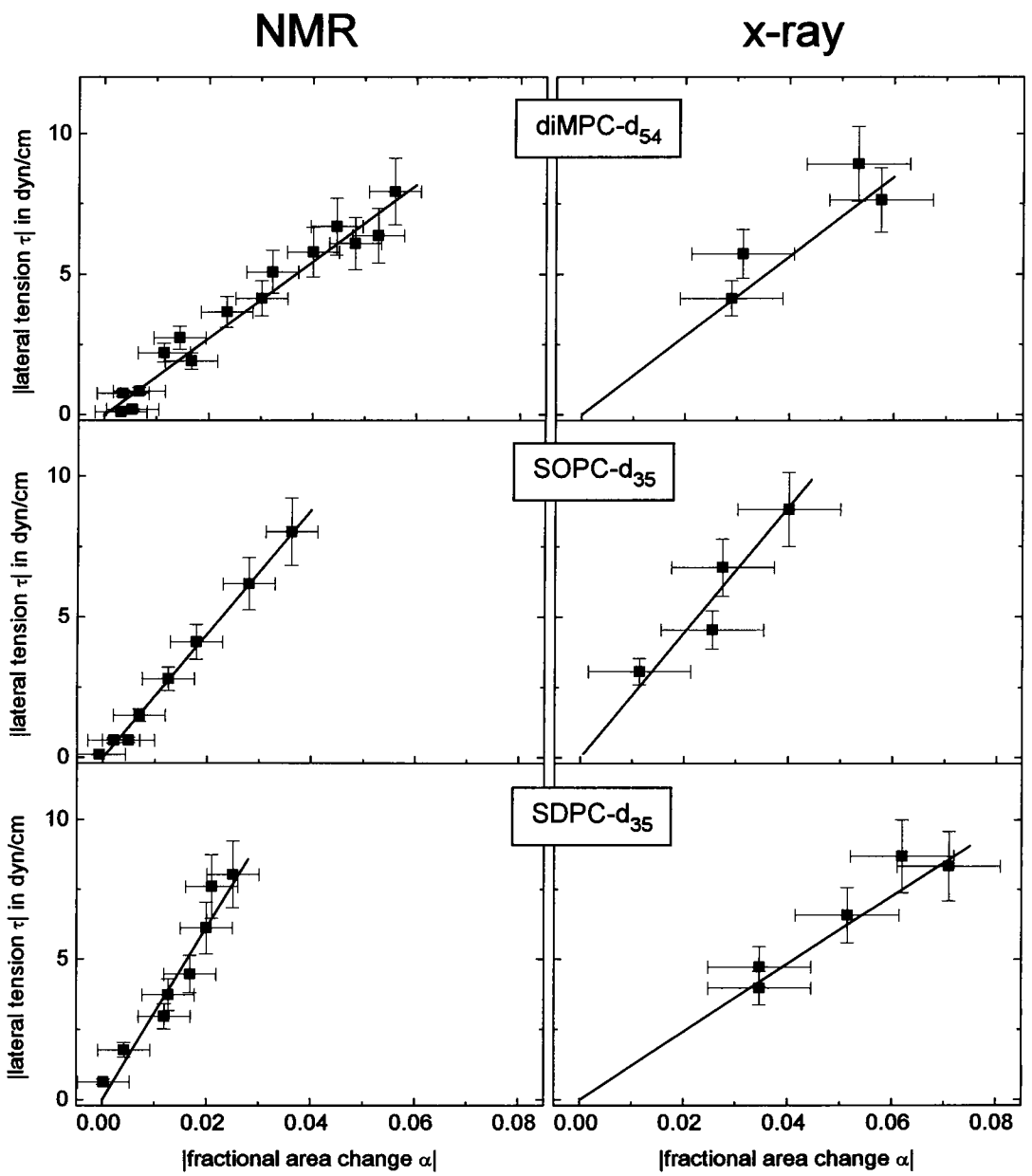


FIGURE 7 Lateral pressure in the bilayer, $\tau$, as a function of fractional area change, $\alpha$, calculated from $^2$H-NMR (*left side*) and x-ray diffraction data (*right side*), respectively. The NMR data display a linear relationship between $\alpha$ and $\tau$ over the entire range studied. In contrast, analysis of the x-ray data was restricted to samples with low water content ($R_{W/L} < 15$) to obtain meaningful $\alpha$ values. In this range, a linear relation is found for the x-ray data, too. The slope of each individual regression line corresponds to a $K_a$ value. NMR data reflect the compressibility of the saturated, perdeuterated, acyl chains while x-ray data characterize the compressibility of the entire bilayer. The larger error bars of the fractional area change $\alpha$ in the x-ray data set is due to the dependency of $A^{x\text{-}ray}$ on both $d$ and $R_{W/L}$, while $A^{NMR}$ is a function of one experimental quantity, $\langle S \rangle$, only.

area values (i.e., at high water content) would seriously obscure the linear elastic response of the bilayer to lateral pressure.

## Polyunsaturation and membrane deformations

The docosahexaenoic acid containing SDPC-$d_{35}$ bilayer has the lowest area compressibility modulus of the three investigated phospholipids. Based on the area compressibility moduli, $K_a$, and the cross-sectional area in excess water, $A_0$, of both the (18:0) chain ($K_a$ = 307 dyn/cm, $A_0$ = 31.9 Å$^2$) and the entire SDPC-$d_{35}$ molecule ($K_a$ = 121 dyn/cm, $A_0$ = 69.2 Å$^2$) we estimated a $K_a$ = 80 dyn/cm for the polyunsaturated (22:6n3) chain. We have to stress the tentative nature of this estimate. Additivity of lateral compressibility of the individual acyl chains was assumed, which may or may not be justified. The estimated $K_a$ refers to (22:6n3) chains in a SDPC matrix and perhaps does not represent a material constant of the (22:6n3) chain. An investigation of elastic properties of di-22:6n3 PC is in progress.

Larger membrane free volume in polyunsaturated bilayers, which may translate into lower lateral compressibility moduli, was observed previously by Straume and Litman (1987b) in experiments on a series of lipid bilayers with varying degrees of unsaturation by time-resolved fluorescence polarization measurements on DPH. Peculiarly high lateral compressibility (low compressibility modulus, $K_a$) of polyunsaturated lipids may be important for the membrane's ability to accommodate conformational changes of integral proteins. This is evidenced by the finding that the ability of rhodopsin to achieve its functionally active conformation, meta II, is correlated with increased bilayer free volume (Mitchell et al., 1992). It has been speculated that the meta I–meta II transition is related to a lateral expansion of rhodopsin in the membrane (Liebman et al., 1987; Dratz and Holte, 1992). However, an increase in cross-sectional area of the protein does not result automatically in lateral compression of the surrounding lipid molecules. Instead, the entire membrane could expand laterally or bulge to accommodate the area increase. Nevertheless, it is likely that lateral area compression of the lipid matrix is of functional importance because 1) lateral expansion of the membrane may be restricted by a protein belt around lipid domains, and 2) bulging may be suppressed by interactions between neighboring lipid layers. Furthermore, 3) it is conceivable that fast structural transitions of proteins may result in a transient compression of the surrounding lipid annulus with slow relaxation of this pressure by lateral expansion and bulging. Indeed, the meta I–meta II transition of rhodopsin has a rate constant of milliseconds (Hofmann, 1986) while size and shape changes of lipidic particles take milliseconds to seconds (Faucon et al., 1989).

## Area compressibility versus expansivity of membranes

The range of membrane area expansion accessible with micromechanical manipulation of liposomes is limited by the eventual rupture of the liposome upon increase of bilayer tension. Vesicle lysis occurs at 2–3 dyn/cm and 5.7 ± 0.02 dyn/cm for diMPC and SOPC in the $L_\alpha$ phase, respectively (Evans and Needham, 1987; Needham and Nunn, 1990). Polyunsaturation of the acyl chains is known to further decrease mechanical stability of liposomes (Needham and Nunn, 1990). In the area compression regime, membrane compressibility can be studied over a larger range of lateral tension. The value of $\tau$ is proportional to $\alpha$ over the entire range of lateral pressures accessible with PEG solutions for the three lipids investigated (Fig. 7), i.e., the bilayer elasticity limit for compression must be beyond 8 dyn/cm. We anticipate an increase of $K_a$ for membranes at very high osmotic stress, corresponding to $R_{W/L} \ll 10$, in analogy to compressibility behavior of lipid monolayers (Demel et al., 1972; Ghosh et al., 1973; Marsh, 1996).

The $K_a$ values obtained at 30°C in this study are reasonably close to elastic area expansion moduli determined with micromechanical manipulation on single-walled large liposomes of diMPC [145 dyn/cm at 29°C (Evans and Needham, 1987)] and SOPC [200 dyn/cm (Evans and Needham, 1987) and 193 dyn/cm (Needham and Nunn, 1990) at $T$ = 15°C].

Micromechanical manipulation experiments are performed on single-walled liposomes while osmotic stress experiments are conducted on multilamellar liposomes. However, $K_a$ values are identical within experimental error. This suggests that interbilayer forces have only negligible influence on lateral compressibility over the investigated range of osmotic stress.

Some caution must be exercised when using absolute values for $K_a$. Quantitative measurements by the OS method require a very accurate calibration curve for water activity versus polymer concentration. For PEG solutions, such curves have been measured at a number of laboratories [see, e.g., Parsegian et al. (1986); Gawrisch et al. (1988); Hasse et al. (1995)] and the calibration curves differ somewhat. We used data from Rand's laboratory obtained on PEG with similar molecular weight distribution at the temperature of our experiments, 30°C (Parsegian et al., 1986). Nevertheless, we consider the PEG calibration curve to be the single most important source for a systematic error in the $K_a$ values determined by the OS method. Relative differences between $K_a$ values are not affected by this uncertainty.

## Repulsive forces between bilayers and flexibility

In the range of osmotic pressure, $\Pi$, where the Luzzati approach is applicable, a linear relation between ln $\Pi$ and $d_W$ was found for all three lipids. The interbilayer pressure was fitted to $P_0 \exp(-d_W/\lambda)$. The hydration force parameters, $\lambda$ and $P_0$ (Table 1), were obtained by linear regression of data points measured at low water content, i.e., $R_{W/L} \leq 14$. These values are reasonably close to literature data for diMPC at 27°C ($\lambda$ = 2.16 Å, log $P_0$ = 10.49) and SOPC at 30°C ($\lambda$ = 1.98 Å, log $P_0$ = 10.51), which have been compressibility adjusted (Rand et al., 1988; Rand and Parsegian, 1989). This is a procedure in which the known lateral compressibility modulus of a lipid bilayer is used to calculate changes in bilayer thickness when subjected to osmotic stress (Rand et al., 1988). SDPC-$d_{35}$ has a longer decay length, $\lambda$, and a smaller prefactor, $P_0$, of the hydration force than the other two lipids studied.

At low hydration the repeat spacing, $d$, measured for SDPC-$d_{35}$ is intermediate between diMPC-$d_{54}$ and SOPC-$d_{35}$, while in excess water the spacing is largest for SDPC-$d_{35}$ ($d$ = 66.2 Å), indicating that the water layer between

**TABLE 1 Hydration force parameters at 30°C**

| | λ/Å | log $P_0$/dyn/cm |
|---|---|---|
| diMPC-$d_{54}$ | 2.5 ± 0.4 | 9.7 ± 0.3 |
| SOPC-$d_{35}$ | 2.3 ± 0.2 | 9.8 ± 0.2 |
| SDPC-$d_{35}$ | 2.9 ± 0.2 | 9.4 ± 0.2 |

opposing bilayers is significantly thicker for SDPC-$d_{35}$ (Fig. 8).

It has been shown that an increased disorder in lipid headgroups, which can be induced by increased disorder in the chains, typically leads to stronger hydration, a longer hydration force decay length, $\lambda$, and decreasing $P_0$ (Leikin et al., 1993). Increased repulsion between SDPC-$d_{35}$ bilayers with polyunsaturated chains in excess water could also come from stronger undulatory fluctuations (Helfrich, 1978; Evans and Parsegian, 1986) resulting from a smaller bending rigidity modulus, $k_c$, of the thinner bilayer (Evans and Rawicz, 1990). Indeed, for the polyunsaturated lipid diarachidonylphosphatidylcholine, low values for the elastic moduli, $K_a$ and $k_c$, (Needham and Nunn, 1990; Evans and Rawicz, 1990) as well as large values for $A$ and the interbilayer fluid spacing in excess water (McIntosh et al., 1995) have been reported.

## SUMMARY

The osmotic stress technique along with structural data from NMR and x-ray diffraction is well suited to study lateral compressibility of lipid membranes in the $L_\alpha$ phase. Combining structural parameters from NMR and diffraction methods allows one to differentiate between the response of the entire bilayer to lateral pressure and of individual deuterium-labeled fatty acid chains. The saturated chain in SDPC-$d_{35}$ appears to be less compressible than the docosahexaenoic acid chain, highlighting the distinct properties that polyunsaturation may impart on a bilayer.

Increasing the number of double bonds in the *sn*-2 chain from one in SOPC-$d_{35}$ to six in SDPC-$d_{35}$ results in lower orientational order of the stearoyl chain, a thinner bilayer, an increased area per lipid molecule, enhanced adsorption of water, and a thicker water layer between opposing lipid bilayers in excess water. Polyunsaturation reduces energy requirements for elastic deformation of the bilayer.

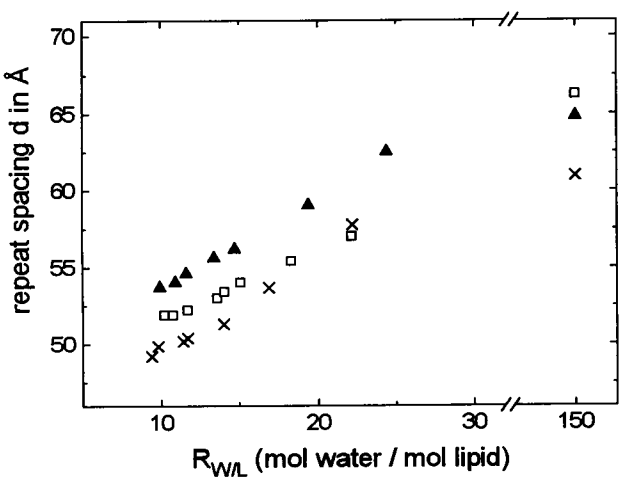


FIGURE 8 Lamellar repeat spacing, $d$, of multilamellar membrane stacks as a function of molar water-to-lipid ratio, $R_{W/L}$, measured at 30°C. Data for diMPC-$d_{54}$ (×), SOPC-$d_{35}$ (▲), and SDPC-$d_{35}$ (□) are shown.

## APPENDIX

Detailed accounts on application of the osmotic stress technique in combination with x-ray diffraction for characterization of the elastic area compressibility modulus of membranes have been published previously (Parsegian et al., 1979; Evans and Skalak, 1980). A brief summary of the method is given below.

The membrane is treated in terms of a unit cell, consisting of two lipids and 2 × $R_{W/L}$ water molecules. The total volumes of water and lipid in the unit cell are $V_W$ and $V_L$, respectively. The height of the unit cell corresponds to the repeat spacing, $d$, of the multi-bilayer membrane stack and the cross-sectional area is $A$. The repeat spacing is divided into water and lipid layer thicknesses, $d_W$ and $d_L$, respectively, based on the gravimetric method suggested by Luzzati (Luzzati, 1968; Rand et al., 1988).

Equilibration of a bilayer stack at a given osmotic pressure, $\Pi$, lowers $V_W$ and increases the free energy, $G$, of the membrane unit cell with respect to the fully hydrated state.

$$\Delta G = -\Pi \Delta V_W \tag{15}$$

The induced reduction in volume ($\Delta V_W$) will be compensated for by changes of the dimensions of both the lipid and water compartments of the unit cell.

$$\Delta V_W = (d_L + d_W)\Delta A + A\Delta(d_L + d_W) \tag{16}$$

Since the lipids are volumetrically nearly incompressible (Cevc and Marsh, 1987), i.e., $d_L\ \Delta A + A\ \Delta d_L = 0$, combination of Eqs. 15 and 16 gives:

$$\Delta G = -\Pi d_W \Delta A - \Pi A \Delta d_W. \tag{17}$$

The isothermal partial derivative of $G$ over $A$ or $d_W$ gives the isotropic lateral tension, $\tau$, and the force acting perpendicular to the lipid/water interface, $F_\perp$, respectively, if changes in $A$ and $d_W$ are assumed to be independent from each other.

$$\left(\frac{\partial G}{\partial A}\right)_{T,dw} = -\Pi d_W \equiv \tau \tag{18}$$

$$\left(\frac{\partial G}{\partial d_W}\right)_{T,A} = -\Pi A \equiv F_\perp \tag{19}$$

Osmotic stress has been widely used to study repulsive hydration forces between bilayers according to Eq. 19 (Parsegian et al., 1979; Rand and Parsegian, 1989). However, it also provides a means to investigate the response of the bilayer to lateral tension, $\tau$, according to Eq. 18. Using $d_W = V_W/A = 2\ R_{W/L}\ v_W/A$, where $v_W$ is the molecular volume of water, Eq. 18 can be rewritten as:

$$\tau = -2v_W \frac{R_{W/L}}{A}\Pi \tag{20}$$

Measurement of the area per lipid molecule, $A$, and the water content of the unit cell, $R_{W/L}$, as a function of osmotic pressure, $\Pi$, allows the determination of the elastic isothermal area compressibility modulus, $K_a$, of the bilayer.

We thank Laura Holte for help with the experiments and many discussions, Nils Olsson for checking lipid purity by HPLC, and Leepo Yu and Gary Melvin for their support enabling the x-ray experiments. We acknowledge useful discussions with Burton Litman, John Nagle, Adrian Parsegian, and Peter Rand.

## REFERENCES


Attwood, P. V., and H. Gutfreund. 1980. The application of pressure relaxation to the study of the equilibrium between metarhodopsin I and II from bovine retinas. *FEBS Lett.* 119:323–326.

Bunn, C. W. 1939. The crystal structure of long-chain normal paraffin hydrocarbons. The "shape" of the $>CH_2$ group. *Trans. Faraday Soc.* 35:482–491.

Cevc, G., and D. Marsh. 1987. Phospholipid Bilayers. Physical Principles and Models. John Wiley & Sons, Inc., New York.

Davis, J. H. 1983. The description of membrane lipid conformation, order and dynamics by $^2$H-NMR. *Biochim. Biophys. Acta.* 737:117–171.

Demel, R. A., W. S. M. Geurts van Kessel, and L. L. M. Van Deenen. 1972. The properties of polyunsaturated lecithins in monolayers and liposomes and the interactions of these lecithins with cholesterol. *Biochim. Biophys. Acta.* 266:26–40.

Dratz, E. A., and A. J. Deese. 1986. The role of docosahexaenoic acid in biological membranes: examples from photoreceptors and model membrane bilayers. *In* Health Effects of Polyunsaturated Fatty Acids in Seafoods. A. P. Simopolous, R. R. Kifer, and R. E. Martin, editors. Academic Press, New York. 319–351.

Dratz, E. A., and L. L. Holte. 1992. The "molecular spring" model for the function of 22:6$\omega$3 in biological membranes. *In* Essential Fatty Acids and Eicosanoids: Invited Papers from the Third International Congress. A. F. Sinclair and R. A. Gibson, editors. American Oil Chemists Society, Champaign, IL. 122–127.

Duwe, H. P., J. Kaes, and E. Sackmann. 1990. Bending elastic moduli of lipid bilayers: modulation by solutes. *J. Phys. France.* 51:945–962.

Evans, E., and R. Kwok. 1982. Mechanical calorimetry of large dimyristoylphosphatidylcholine vesicles in the phase transition region. *Biochemistry.* 21:4874–4879.

Evans, E., and D. Needham. 1987. Physical properties of surfactant bilayer membranes: thermal transitions, elasticity, rigidity, cohesion, and colloidal interactions. *J. Phys. Chem.* 91:4219–4228.

Evans, E. A., and V. A. Parsegian. 1986. Thermal-mechanical fluctuations enhance repulsion between bimolecular layers. *Proc. Natl. Acad. Sci. USA.* 83:7132–7136.

Evans, E., and W. Rawicz. 1990. Entropy-driven tension and bending elasticity in condensed-fluid membranes. *Phys. Rev. Lett.* 64: 2094–2097.

Evans, E. A., and R. Skalak. 1980. Mechanics and Thermodynamics of Biomembranes. CRC Press, Inc., Boca Raton, FL.

Faucon, J. F., M. D. Mitov, P. Méléard, I. Bivas, and P. Bothorel. 1989. Bending elasticity and thermal fluctuations of lipid membranes. Theoretical and experimental requirements. *J. Phys. France.* 50:2389–2414.

Gawrisch, K., K. Arnold, K. Dietze, and U. Schulze. 1988. Hydration forces between phospholipid membranes and the polyethylene glycol induced membrane approach. *In* Electromagnetic Fields and Biomembranes. M. Markov and M. Blank, editors. Plenum Press, New York. 9–18.

Gawrisch, K., W. Richter, A. Möps, P. Balgavy, K. Arnold, and G. Klose. 1985. The influence of water concentration on the structure of egg yolk phospholipid/water dispersions. *Studia Biophys.* 108:5–16.

Ghosh, D., M. A. Williams, and J. Tinoco. 1973. The influence of lecithin structure on their monolayer behavior and interactions with cholesterol. *Biochim. Biophys. Acta.* 291:351–362.

Hasse, H., H. P. Kany, R. Tintinger, and G. Maurer. 1995. Osmotic virial coefficients of aqueous poly(ethylene glycol) from laser-light scattering and isopiestic measurements. *Macromolecules.* 28:3540–3552.

Helfrich, W. 1978. Steric interaction of fluid membranes in multilayer systems. *Z. Naturforsch.* 33a:305–315.

Hofmann, K. P. 1986. Photoproducts of rhodopsin in the disc membrane. *Photobiochem. Photobiophys.* 13:309–327.

Holte, L. L., S. A. Peter, T. M. Sinnwell, and K. Gawrisch. 1995. $^2$H-nuclear magnetic resonance order parameter profiles suggest a change of molecular shape for phosphatidylcholines containing a polyunsaturated acyl chain. *Biophys. J.* 68:2396–2403.

Holte, L. L., F. Separovic, and K. Gawrisch. 1996. Nuclear magnetic resonance investigation of hydrocarbon chain packing in bilayers of polyunsaturated phospholipids. *Lipids.* 31:S199–S203.

Ipsen, J. H., O. G. Mouritsen, and M. Bloom. 1990. Relationships between lipid membrane area, hydrophobic thickness, and acyl-chain orientational order. The effects of cholesterol. *Biophys. J.* 57:405–412.

Jendrasiak, G. L., and J. H. Hasty. 1974. The hydration of phospholipids. *Biochim. Biophys. Acta.* 337:79–91.

Johnson, M. L. 1985. The analysis of ligand-binding data with experimental uncertainties in the independent variables. *Anal. Biochem.* 148: 471–478.

Johnson, M. L., and S. G. Frasier. 1985. Nonlinear least-squares analysis. *Methods Enzymol.* 117:301–343.

Klose, G., B. König, H. W. Meyer, G. Schulze, and G. Degovics. 1988. Small-angle x-ray scattering and electron microscopy of crude dispersions of swelling lipids and the influence of the morphology on the repeat distance. *Chem. Phys. Lipids.* 47:225–234.

Klose, G., B. König, and F. Paltauf. 1992. Sorption isotherms and swelling of POPC in $H_2O$ and $^2H_2O$. *Chem. Phys. Lipids.* 61:265–270.

Kwok, R., and E. Evans. 1981. Thermoelasticity of large lecithin bilayer vesicles. *Biophys. J.* 35:637–652.

Lafleur, M., B. Fine, E. Sternin, P. R. Cullis, and M. Bloom. 1989. Smoothed orientational order profile of lipid bilayers by $^2$H-nuclear magnetic resonance. *Biophys. J.* 56:1037–1041.

Lamola, A. A., T. Yamane, and A. Zipp. 1974. Effects of detergents and high pressures upon the metarhodopsin I–metarhodopsin II equilibrium. *Biochemistry.* 13:738–745.

Leikin, S., V. A. Parsegian, D. C. Rau, and R. P. Rand. 1993. Hydration forces. *Annu. Rev. Phys. Chem.* 44:369–395.

Liebman, P. A., K. R. Parker, and E. A. Dratz. 1987. The molecular mechanism of visual excitation and its relation to the structure and composition of the rod outer segment. *Annu. Rev. Physiol.* 49:765–791.

Lis, L. J., M. McAlister, N. Fuller, and R. P. Rand. 1982. Measurement of the lateral compressibility of several phospholipid bilayers. *Biophys. J.* 37:667–672.

Litman, B. J., and D. C. Mitchell. 1996. A role for phospholipid polyunsaturation in modulating membrane protein function. *Lipids.* 31: S193–S197.

Luzzati, V. 1968. X-ray diffraction studies of lipid-water systems. *In* Biological Membranes, Vol. 1. D. Chapman, editor. Academic Press, London. 71–123.

Marsh, D. 1992. CRC Handbook of Lipid Bilayers. CRC Press, Inc., Boca Raton, FL.

Marsh, D. 1996. Lateral pressure in membranes. *Biochim. Biophys. Acta.* 1286:183–223.

McCabe, M. A., and S. R. Wassall. 1995. Fast-Fourier-transform dePaking. *J. Magn. Reson. B.* 106:80–82.

McGee, C. D., and C. E. Greenwood. 1989. Effects of dietary fatty acid composition on macronutrient selection and synaptosomal fatty acid composition in rats. *Lipids.* 24:1561–1568.

McIntosh, T. J., S. Advani, R. E. Burton, D. V. Zhelev, D. Needham, and S. A. Simon. 1995. Experimental tests for protrusion and undulation pressures in phospholipid bilayers. *Biochemistry.* 34:8520–8532.

McIntosh, T. J., and S. A. Simon. 1986. Hydration force and bilayer deformation: a reevaluation. *Biochemistry.* 25:4058–4066.

Miljanich, G. P., L. A. Sklar, D. L. White, and E. A. Dratz. 1979. Disaturated and dipolyunsaturated phospholipids in the bovine retinal rod outer segment disk membrane. *Biochim. Biophys. Acta.* 552: 294–306.

Mitchell, D. C., M. Straume, and B. J. Litman. 1992. Role of *sn*-1-saturated, *sn*-2-polyunsaturated phospholipids in control of membrane receptor conformational equilibrium: effects of cholesterol and acyl chain unsaturation on the metarhodopsin I-metarhodopsin II equilibrium. *Biochemistry.* 31:662–670.

Morrow, M. R., J. P. Whitehead, and D. Lu. 1992. Chain-length dependence of lipid bilayer properties near the liquid crystal to gel phase transition. *Biophys. J.* 63:18–27.

Nagle, J. F. 1993. Area/lipid of bilayers from NMR. *Biophys. J.* 64: 1476–1481.

Nagle, J. F., and D. A. Wilkinson. 1978. Lecithin bilayers. Density measurements and molecular interactions. *Biophys. J.* 23:159–175.

Nagle, J. F., R. Zhang, S. Tristram-Nagle, W. Sun, and H. I. Petrache. 1996. X-ray structure determination of fully hydrated $L_\alpha$ phase dipalmitoylphosphatidylcholine bilayers. *Biophys. J.* 70:1419–1431.

Needham, D. 1995. Cohesion and permeability of lipid bilayer vesicles. *In* Permeability and Stability of Lipid Bilayers. E. A. Disalvo and S. A. Simon, editors. CRC Press, Inc., Boca Raton, FL. 49–76.

Needham, D., and E. Evans. 1988. Structure and mechanical properties of giant lipid (DMPC) vesicle bilayers from 20°C below to 10°C above the liquid crystal-crystalline phase transition at 24°C. *Biochemistry.* 27: 8261–8269.

Needham, D., and R. S. Nunn. 1990. Elastic deformation and failure of lipid bilayer membranes containing cholesterol. *Biophys. J.* 58: 997–1009.

O'Brian, D. F., L. F. Costa, and R. A. Ott. 1977. Photochemical functionality of rhodopsin-phospholipid recombinant membranes. *Biochemistry.* 16:1295–1303.

Parsegian, V. A., N. Fuller, and R. P. Rand. 1979. Measured work of deformation and repulsion of lecithin bilayers. *Proc. Natl. Acad. Sci. USA.* 76:2750–2754.

Parsegian, V. A., R. P. Rand, N. L. Fuller, and D. C. Rau. 1986. Osmotic stress for the direct measurement of intermolecular forces. *Methods Enzymol.* 127:400–416.

Rand, R. P., N. Fuller, V. A. Parsegian, and D. C. Rau. 1988. Variation in hydration forces between neutral phospholipid bilayers: evidence for hydration attraction. *Biochemistry.* 27:7711–7722.

Rand, R. P., and V. A. Parsegian. 1989. Hydration forces between phospholipid bilayers. *Biochim. Biophys. Acta.* 988:351–376.

Salmon, A., S. W. Dodd, G. D. Williams, J. M. Beach, and M. F. Brown. 1987. Configurational statistics of acyl chains in polyunsaturated lipid bilayers from $^2$H-NMR. *J. Am. Chem. Soc.* 109:2600–2609.

Schindler, H., and J. Seelig. 1975. Deuterium order parameters in relation to thermodynamic properties of a phospholipid bilayer. A statistical mechanical interpretation. *Biochemistry.* 14:2283–2287.

Schneider, M. B., J. T. Jenkins, and W. W. Webb. 1984. Thermal fluctuations of large cylindrical phospholipid vesicles. *Biophys. J.* 45: 891–899.

Seelig, J. 1977. Deuterium magnetic resonance: theory and application to lipid membranes. *Q. Rev. Biophys.* 10:353–418.

Seelig, A., and J. Seelig. 1974. The dynamic structure of fatty acyl chains in a phospholipid bilayer measured by deuterium magnetic resonance. *Biochemistry.* 13:4839–4845.

Seelig, J., and A. Seelig. 1980. Lipid conformation in model membranes and biological membranes. *Q. Rev. Biophys.* 13:19–61.

Servuss, R. M., W. Harbich, and W. Helfrich. 1976. Measurement of the curvature-elastic modulus of egg lecithin bilayers. *Biochim. Biophys. Acta.* 436:900–903.

Sternin, E., M. Bloom, and A. L. MacKay. 1983. De-Paking of NMR spectra. *J. Magn. Reson.* 55:274–282.

Straume, M., and B. J. Litman. 1987a. Influence of cholesterol on equilibrium and dynamic bilayer structure of unsaturated acyl chain phosphatidylcholine vesicles as determined from higher order analysis of fluorescence anisotropy decay. *Biochemistry.* 26:5121–5126.

Straume, M., and B. J. Litman. 1987b. Equilibrium and dynamic structure of large, unilamellar, unsaturated acyl chain phosphatidylcholine vesicles. Higher order analysis of 1,6-diphenyl-1,3,5-hexatriene and 1-[4-(trimethylammonio)phenyl-6-phenyl]-1,3,5-hexatriene anisotropy decay. *Biochemistry.* 26:5133–5120.

Wattenberg, B. 1992. Vesicular traffic in eukaryotic cells. *In* The Structure of Biological Membranes. P. Yeagle, editor. CRC Press, Inc., Boca Raton, FL. 997–1046.

White, S., R. E. Jacobs, and G. I. King. 1987. Partial specific volumes of lipid and water in mixtures of egg lecithin and water. *Biophys. J.* 52:663–665.

Wiedmann, T. S., R. D. Pates, J. M. Beach, A. Salmon, and M. F. Brown. 1988. Lipid-protein interactions mediate the photochemical function of rhodopsin. *Biochemistry.* 27:6469–6474.

Wiener, M. C., and S. H. White. 1991. Fluid bilayer structure determination by the combined use of x-ray and neutron diffraction. I. Fluid bilayer models and the limits of resolution. *Biophys. J.* 59:162–173.